# We are IntechOpen, the world's leading publisher of Open Access books Built by scientists, for scientists

**4,800**
Open access books available

**122,000**
International authors and editors

**135M**
Downloads

Our authors are among the

**154**
Countries delivered to

**TOP 1%**
most cited scientists

**12.2%**
Contributors from top 500 universities

CLARIVATE ANALYTICS BOOK CITATION INDEX INDEXED

WEB OF SCIENCE™

Selection of our books indexed in the Book Citation Index in Web of Science™ Core Collection (BKCI)

## Interested in publishing with us?
## Contact book.department@intechopen.com

Numbers displayed above are based on latest data collected.
For more information visit www.intechopen.com

Chapter

# Nanostructures in Dye-Sensitized and Perovskite Solar Cells

*Shoyebmohamad F. Shaikh, Nanasaheb M. Shinde, Damin Lee, Abdullah M. Al-Enizi, Kwang Ho Kim and Rajaram S. Mane*

## Abstract

Due to increase of attention in energy and environmental concerns, there has been much interest developed in clean and renewable energy technologies. The utilization of green and eco-friendly sunlight through solar cells like photovoltaic cells, photo-electrochemical cells, and dye-sensitize and perovskite solar cells (DSSCs and PSCs) produces energy demand. Due to high electron mobility, suitable band alignment, and high optical transparency, the binary and ternary transition metal oxide materials such as $TiO_2$, $SnO_2$, ZnO, $WO_3$, $Bi_2O_3$ and $SrTiO_3$, $Zn_2SnO_4$, $BaSnO_3$, etc. have attracted considerable attention as DSSC and PSC electrode materials. Highly efficient solar cells with sustainable performance under severe mechanical deformations are in great demand in forming wearable power supply devices, essential for space technologies. In this regard, myriads of studies have progressed in developing the said metal oxides by various means of nanostructure forms. The aim of this chapter is to highlight research background, basic concepts, operating parameters, working principles, theoretical aspects, and selection of materials with essential properties for DSSCs and PSCs applications.

**Keywords:** nanostructures, binary and ternary metal oxides, photovoltaic, dye-sensitized solar cells, perovskite solar cells

## 1. Introduction

### 1.1 Background and motivation

The predicted global energy needs, due to increasing concerns of environmental pollution in the twenty-first century, have motivated a great deal of efforts into the reduction of fossil fuel consumption followed exploration of clean, renewable, abundant, and eco-friendly renewable energy source technologies to enrich the quality of lives on this planet. Several renewable energy technologies are being investigated to evaluate their potential to address growing demand. These sources include wind turbines, hydropower, nuclear power plants, wave and tidal power, solar cells, solar thermal, and so on. Among these sources, photovoltaic technology, where sunlight is converted into an electrical energy, the so-called solar energy, has drawn considerable attention as it converts into a unique and potential solution. All renewable energy source technologies confirm a common dream, i.e., to capture one type of energy which later can convert into valuable and strategically important asset, that is, electric

energy. As the Sun provides a considerable amount of energy for our planet, the energy it provided is approximately 10,000 times more than global demand (i.e., 31,024 J/year); conversion of its 0.1% that is received by the Earth's surface using solar cells with power conversion efficiency of 10% would fulfill our present needs [1].

## 1.2 Photovoltaic cell

Photovoltaic device generates electrical power by converting sunlight into electricity in the presence of semiconducting materials using the phenomenon, the so-called photovoltaic effect. At first, French scientist Alexandre Becquerel in 1839 discovered photovoltaic effect [2]. After that more than 100 years later, Reynolds et al. in 1954 developed silicon solar cell that was primarily used in space applications until about the mid-1970s [3]. Recently, various kinds of photovoltaic devices are being developed, including silicon solar cells (Si-SCs), dye-sensitized solar cells (DSSCs), quantum dot-sensitized solar cells (QD-DSSCs), organic photovoltaic cells (OPVs), perovskite solar cells (PSCs), etc. Presently, solar cell devices are being used in customer electronics, small-scale remote residential power systems, communications, and signaling applications.

## 1.3 Photovoltaic parameters

In addition to series and shunt resistance, the photovoltaic solar cells' performance is mainly characterized by six important parameters, (1) short-circuit current density, (2) open-circuit voltage, (3) maximum power output, (4) fill factor, (5) incident photon-to-current conversion efficiency, and (6) solar energy to power conversion efficiency, which are thoroughly discussed as follows [4].

### *1.3.1 Short-circuit current density*

The short-circuit current density is usually written as $J_{sc}$, which corresponds to the current that passes through the solar cell of one square centimeter area when the impedance is low and voltage across solar cell is zero. The $J_{sc}$ arises due to generation and collection of light-generated charge carriers. For ideal solar cell, at most moderate resistive loss mechanisms, the $J_{sc}$ and light-generated current are identical. Basically, $J_{sc}$ depends upon the area of the solar cell, number of photons reaching at the junction, exposure of incident light, etc.

### *1.3.2 Open-circuit voltage*

The open-circuit voltage is usually presented as $V_{oc}$, which is the maximum voltage generated from a solar cell when there is no current. The $V_{oc}$ corresponds to the amount of forward bias on solar cell due to bias of solar cell junction with light-generated current. The power ($P$) produced by solar cell in Watt can be easily calculated alone by $I$-$V$ curve using the equation, $P = IV$. The voltage and current at maximum power from point are denoted as $V_{mp}$ and $I_{mp}$, respectively.

### *1.3.3 Maximum power output*

For a given bias voltage, the power output of solar cell is the product of measured cell current and voltage. The $J_{sc}$ and $V_{oc}$ are the maximum current and voltage, respectively, from a solar cell. However, at both of these operating points, the power from solar cell is zero.

### *1.3.4 Fill factor*

The fill factor (*ff*) is defined as the ratio of the maximum power from the solar cell to the product of $V_{oc}$ and $J_{sc}$. Graphically, *ff* is a measure of "squareness" of solar cell and also an area of the largest rectangle which will fit in the *I-V* curve. Typically, the range of *ff* is from 0.50 to 0.82 or 50 to 82% as the *ff* is also represented in percentage using the following relation:

$$ff(\%) = \frac{P_{mp}}{J_{sc}\,V_{oc}} = \frac{I_{mp}\,V_{mp}}{J_{sc}\,V_{oc}} \times 100 \quad (1)$$

### *1.3.5 Incident photon-to-current conversion efficiency*

The incident monochromatic photon-to-current conversion efficiency (IPCE), sometimes referred to also as the "external quantum efficiency" (EQE), is an important parameter of solar cell device. The IPCE can be under light intensity of 100 mW $cm^2$ (AM1.5), which is estimated in the following equation:

$$IPCE\,(\%) = \frac{J_{sc}(A)}{P(W)} \times \frac{1240}{\lambda(nm)} \times 100 \quad (2)$$

where photocurrent density ($J$) is generated by monochromatic light with wavelength ($\lambda$) and intensity ($P$).

### *1.3.6 Solar-to-electrical power conversion efficiency*

The solar-to-electrical power conversion efficiency ($\eta$%) is an essential parameter to confirm the performance of one solar cell under testing. The $\eta$ is defined as the ratio of energy output from the solar cell to an energy input from the Sun. In addition to reflecting performance of the solar cell itself, $\eta$ depends on the spectrum and intensity of the incident sunlight and temperature of the solar cell. Therefore, terrestrial solar cells are measured under air mass 1.5 conditions in addition to a temperature of 25°C. The solar cells intended for space use are measured under air mass "0" conditions. It is well known that an overall η (%) of the solar cells can be determined by $J_{sc}$, $V_{oc}$, *ff*, and the intensity of the incident light ($P_{in}$) as follows:

$$\eta(\%) = \frac{P_{out}}{P_{in}} = \frac{J_{sc}\,V_{oc}\,ff}{P_{in}} \times 100 \quad (3)$$

## 1.4 History of dye-sensitized and perovskite solar cells

In 1873, Vogel and Berlin invented dye sensitization technique, but until the 1970s DSSCs' mechanism was unclear. Therefore, compared with silicon-based photovoltaic devices, the performance of these early DSSCs was poor ($\eta$ = <1%). The major obstacle in poor performance was relatively low adsorption of dye molecules into the metal oxide photoanode surface. Few improvements in efficiency were achieved by coating a thick layer of dye molecules onto the metal oxide photoanode surface [5]. Nevertheless, the power conversion efficiency was limited to ≤2% due to the low-light harvesting and charge collection from the adsorbed dye molecules. In the 1990s, Prof. Michel Gratzel and his team creatively demonstrated a practical photoelectrochemical cell device with a certified power conversion efficiency of 11.9%,

presenting excellent market competitiveness and commercial prospect [6]. However, such DSSCs of a liquid-state electrolyte are with highly volatile solvents, which not only affect the long-term stability of the device but also limit its large-scale production. In 1998, Gratzel et al. unveiled a solid-state organic hole-transporting material, i.e., 2,2,7,7-tetrakis (N,N-di-p-methoxy-phenylamine)-9,9-spirobifluorene (spiro-OMeTAD), to replace the conventional liquid-state electrolyte for a solid-state DSSCs [7]. From 1998 to 2011, the power conversion efficiency of solid-state DSSCs increased steadily from 0.74% to 7.2% but still much lower than that obtained by liquid-state electrolyte-based DSSCs [8]. In 2009, Miyasaka and co-workers improved the power conversion efficiency of perovskite solar cell to 3.8% by replacing bromine ($MAPbBr_3$) with iodine ($MAPbI_3$) [9]. In 2011, Park et al. prepared $MAPbI_3$ perovskite as quantum dots with a size of ca. 2–3 nm, resulting in an enhanced power conversion efficiency of 6.5% [10]. In the family of photovoltaic device, PSCs have demonstrated much stronger absorption than the standard N719 dye, but the limitation in perovskite-based solar cells was the rapid degradation of the device performance resulting in the dissolution of perovskites in liquid-state electrolytes. In 2012, Park's group works together with Gratzel's group and introduced perovskite-sensitized solar cell by using solid-state spiro-OMeTAD as a hole-transporting material by replacing liquid-state electrolytes [11], where the solid-state spiro-OMeTAD not only solved the problem of perovskite dissolution but also significantly improved the stability and power conversion efficiency (9.7%). Remarkable progress of perovskite solar cell has been made during 2013–2014 as the power conversion efficiency increased to a certified 16.2% and 20.1% [12, 13]. Sahil et al. prepared fully textured monolithic perovskite/silicon tandem solar cells with 25.2% certified power conversion efficiency. Besides the breakthrough in efficiency, novel designs of device architectures aiming for low-cost and highly stable DSSCs and PSCs have also been developed [14].

## 1.5 Theoretical aspect

After the invention of nanostructure-based photovoltaic solar cells, a lot of theoretical and experimental works has been carried out to explain its operation principle. The need for unique theoretical considerations of photovoltaic effect arises from the fundamental differences in the operation between DSSCs and PSCs over traditional semiconductor *p-n and p-i-n* junction solar cells [15].

### *1.5.1 Light absorption*

In photovoltaic solar cell, light absorption and charge transport occur in the same material, whereas in the DSSCs, photons get absorbed by dye molecules and charge transport is carried out in photoanode and electrolyte. The high efficiency of DSSCs is accomplished by coating the internal surfaces of porous metal oxide-based photoanode with special dye (N3, N719, and black dye) molecules which are tuned to absorb incoming photons of all wavelengths. The absorption of a photon by dye molecule takes place *via* an excitation between the electronic states of molecule. Similarly, in PSCs, the absorption spectrum demonstrates good light-harvesting capabilities over the visible to near-IR spectrum which is also stable during prolonged light exposure. For sensitized mesoporous metal oxide devices, it is inferred that after light absorption in the perovskite, electrons are transferred to the metal oxide-based electron transfer layer followed by the conducting substrate (i.e., fluorine-tin-oxide/indium-tin-oxide), and holes are transferred to the spiro-OMeTAD and then to the silver/gold contact electrode for driving the applied load. The enhancement in light absorption near the band edge can be carefully

engineered through various nanostructures for better photon management to increase the current followed by power conversion efficiency.

### *1.5.2 Charge separation*

As the next step of the conversion of light absorption into electrical current, a complete charge separation must be achieved. The charge separation in photovoltaic solar cell is induced by the electric field across the junction, while no such long-range electric fields are found in the DSSCs and PSCs. The charge separation in the DSSCs is basically an electron transfer process from dye molecule to photoanode and hole transport process from oxidized dye to electrolyte. The electron transfer mechanism depends on an electronic structure of dye molecules and energy level matching between the excited state of dye and conduction band of photoanode, i.e., metal oxide. The lowest unoccupied molecular orbital (LUMO) should be above the conduction band edge of photoanode, and the highest occupied molecular orbital (HOMO) should be below the chemical potential of redox pair of electrolyte, i.e., iodide/triiodide, which is supposed to be an energetic driving force for electron and hole separation. In addition, entropic factors play an important role for energetic charge separation. The large density of delocalized states in the metal oxide nanoparticles compared with dye molecules on the surface facilitates electron injection in its conduction band, which eventually increases the driving force in entropy (approximately 0.1 eV) for charge separation. In PSCs, the charge separation and transportation occur between metal oxide as an electron transfer layer and spiro-OMeTAD as a hole transfer layer interfacial surface. On exposing to the Sun's radiation, photo-excited electrons are injected from perovskite absorber layer into the conduction band of the metal oxide electron transfer layer, and the hole is transported to spiro-OMeTAD hole transfer layer followed by the charge collector for driving efficiently.

### *1.5.3 Recombination*

**Figure 1** presents the possible ways of recombination: (1) electron injection from dye-excited state to the conduction band of photoanode, (2) regeneration of dye cation by electron transfer from the redox couple, (3) charge recombination to the cation of dye, (4) recombination to the redox couple, and (5) excited-state decay to the ground state. The photo-injected electrons in the photoanode can have

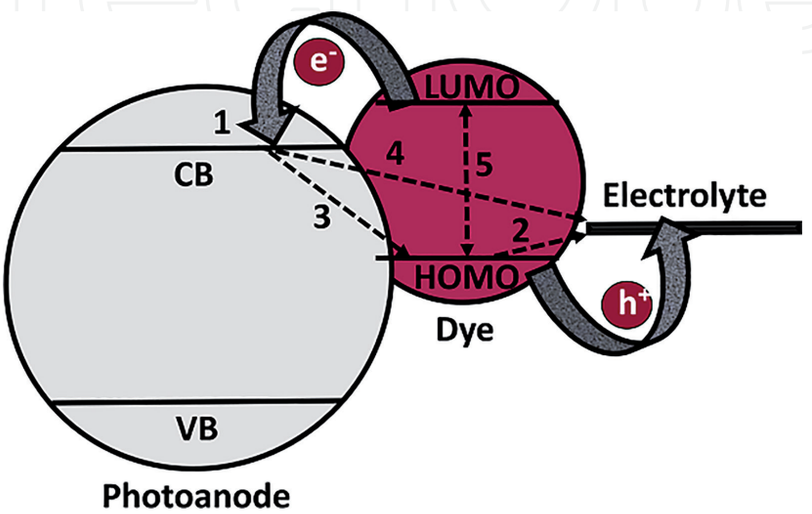


**Figure 1.**
*Plausible electron recombination processes in the DSSCs.*

two possible recombination pathways: direct recombination with the oxidized dyes or with the $I_3^-$ in the electrolyte (**Figure 1**). The latter process is dominant and has thoroughly been studied in the literature by many researches.

*1.5.4 Air mass*

In Astronomy, air mass is direct path length through the earth atmosphere, expressed as a ratio relative to path length vertically upward, i.e., at the zenith. The intensity of solar radiations decreases with distance. Therefore, different air mass standards are being formulated to account for obstruction caused by the Earth's atmosphere.

The air mass standard is denoted by "AM-X" in which X represents air mass coefficient:

$$X = \frac{1}{cos\theta} \tag{4}$$

where $\theta$ is called solar zenith angle. This is defined as the angle between normal of a given point on the earth and light path coming to that point from the Sun. The air mass standards are categorized into three different kinds: briefly, the AM 0 spectrum, for the solar radiation outside the atmosphere; AM 1 for flux of solar energy normal to the Earth; and AM 1.5 represents the solar energy flux impinging at the Earth's surface with 48.2° zenith angle.

## 2. Working principal of the DSSCs

The working principal of the DSSCs is demonstrated in **Figure 2**. The wide bandgap nanocrystalline $TiO_2$ (photoanode) semiconductor film is needed to be deposited on the conducting substrate (FTO) either by direct deposition or by doctor-blade method to provide the necessary large surface area to adsorb sensitizers (dye molecules). Upon absorption of photons, dye molecules are excited from

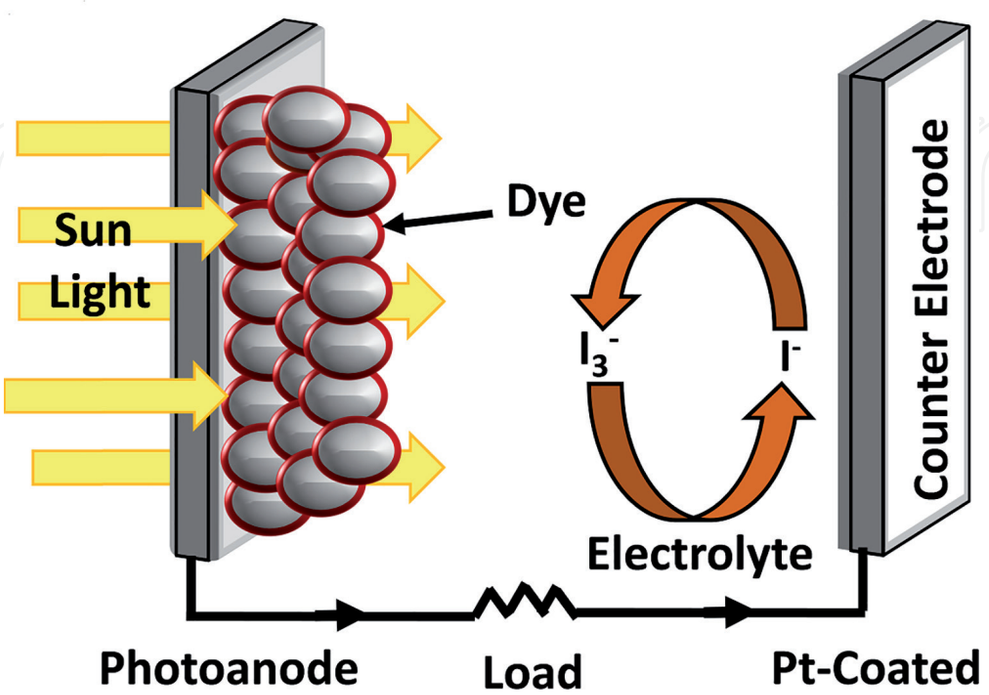


**Figure 2.**
*The operating principle of the DSSCs.*

the HOMO to the LUMO. Once an electron is injected into the conduction band of the $TiO_2$ photoanode, the dye molecule (photosensitizer) is oxidized. The injected electron is then transferred to $TiO_2$ nanostructured photoanode through hopping kinetics which is finally extracted at load, where the work done is delivered as an electrical energy. The electrolytes containing $I^-/I_3^-$ redox ions are used as an electron mediator between the $TiO_2$ photoanode and the platinum-coated counter electrode. Therefore, the oxidized dye molecules (photosensitizer) are regenerated by receiving electrons from the $I^-$ ion redox mediator that get oxidized to $I_3^-$ (triiodide ions) [16]. Regarding the working mechanism of perovskite solar cell, various research groups reported differently; thereby, it is yet to be unprecedented.

## 3. Nanostructures of inorganic materials

A major feature that discriminates various types of nanostructures is their dimensionality (**Figure 3a–d**). The word "nano" stems from the Greek word "nanos," which means dwarf. This word "nano" has been assigned to indicate the number $10^{-9}$, i.e., 1 billionth of any unit [17]. It is believed that the size of particle has inverse relation with the surface area and reactivity thereby, nanoparticles reveal superior practical potential over micron-sized one.

### 3.1 Zero-dimensional nanostructures

The significant progress has been made in the field of zero-dimensional nanostructures. A rich variety of physical and chemical methods have been proposed to synthesize zero-dimensional nanostructures. Recently, zero-dimensional nanostructures such as uniform particle arrays (quantum dots), heterogeneous particle arrays, core-shell quantum dots, onions, and hollow spheres are being obtained by several research groups [18].

### 3.2 One-dimensional nanostructures

In the last decade, one-dimensional nanostructures have stimulated an increasing attention due to their importance in research and a wide range of potential

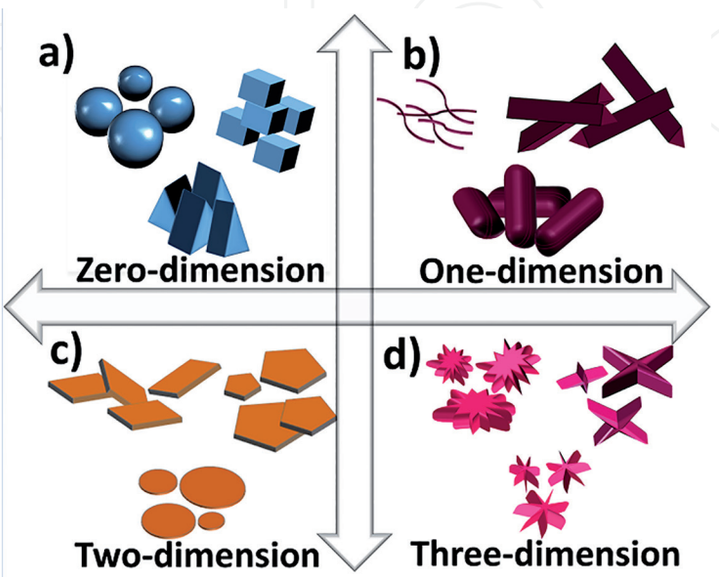


**Figure 3.**
*(a–d) Nanostructures of different dimensions.*

applications. It is generally accepted that one-dimensional nanostructures are ideal for exploring a large number of novel phenomena at the nanoscale level and corroborating the size and dimensionality dependence of functional properties. In **Figure 3b**, one-dimensional nanostructures are endowed with typical spherical, pseudo-spherical, dodecahedral, tetrahedral, octahedral, cubic, and corresponding hollow shapes. One-dimensional nanostructures/morphologies also include nanotubes, nano-needles, nano-rods or nano-wires, nano-shuttles, nano-capsules, hollow structures, etc. [19].

### 3.3 Two-dimensional nanostructures

Two-dimensional nanostructures have two dimensions outside of the nano-metric size range. In recent years, a synthesis of two-dimensional nanostructures with certain geometries exhibits unique shape-dependent characteristics and their subsequent utilization as building blocks for the key components of nano-devices. In **Figure 3c**, two-dimensional nanostructures, such as junctions (continuous islands), branched structures, nano-prisms, nano-plates, nano-sheets, nano-walls, nanodisks, etc., are confirmed in the literature. Round disks, hexagonal/triangular/quadrangular plates or sheets, belts, mesoporous hollow nanospheres, hollow rings, etc. are also forms of two-dimensional nanostructures [20].

### 3.4 Three-dimensional nanostructures

Owing to the large specific surface area and other superior properties over the bulk counterparts arising from the quantum size effect, three-dimensional nanostructures have attracted considerable research interest, and many three-dimensional nanostructures have been synthesized in the past decade (**Figure 3d**). It is well-known that the surface area, shape, size, dimensionality, and morphologies of the nanostructures are key factors to obtain better performance of the device when they are envisaged. As these materials offer higher surface area, they can supply enough absorption sites for all involved molecules in a small space. On the other hand, such materials with higher porosity can lead to a better transportation of dye molecules. A typical three-dimensional nanostructured such as nanocoils, nano-cones, nanoflowers, and nanoballs (dendritic structures) are on a great demand [21].

## 4. Material selection

### 4.1 Binary transition metal oxides

The binary transition metal oxide materials play an important role in the DSSCs and PSCs (**Figure 4a**). Titanium dioxide ($TiO_2$) deserves special attention since its cheap, non-toxicity, abundant, biocompatible, facile preparation with diverse morphologies, stability in both acidic and alkaline media features. The $TiO_2$ exists naturally in three crystalline polymorphs, namely, rutile ($E_g$ = 3.05 eV), anatase ($E_g$ = 3.23 eV), and brookite ($E_g$ = 3.26 eV), and the uniqueness of each lattice structure leads to multifaceted physicochemical and optoelectronic properties [22]. These interesting properties reveal different functionalities, thus influencing their performances in various applications. For instance, rutile phase of $TiO_2$ exhibits a high refractive index and UV absorptivity and is thus capable of being applied in optical communication devices (isolators, modulators, switches, etc.). Meanwhile, anatase is largely preferred in photovoltaics and photocatalysis because of its superior electron mobility, surface chemistry, potentially higher conduction band edge energy, and catalytic activity compared with the other two phases [23]. The problems associated

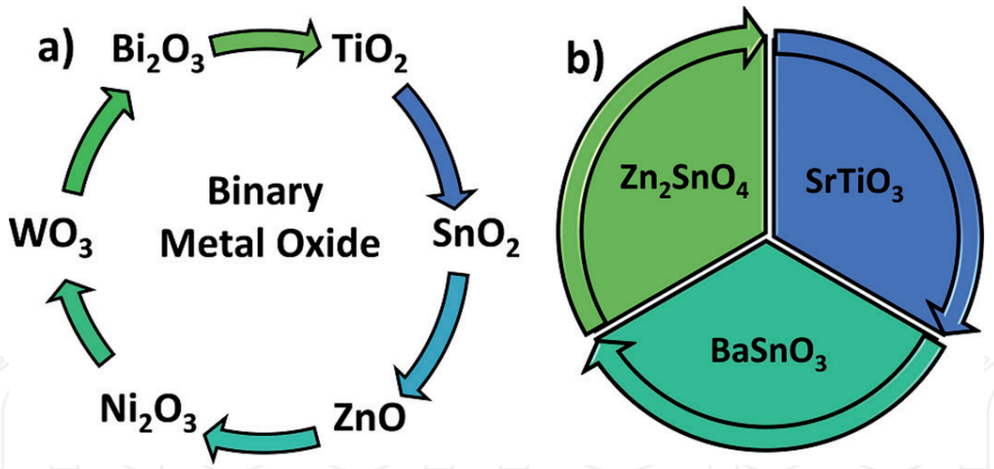


**Figure 4.**
*(a and b) Materials used for the DSSCs and PSCs.*

with $TiO_2$ metal oxide such as high surface state and fast electron recombination rate contribute to adverse effects on the electron mobility and charge transport kinetics. Zinc oxide (ZnO), an important II–VI semiconductor with a wide bandgap of 3.37 eV, similar to $TiO_2$, has high electron mobility (~155–1000 $cm^2\ V^{-1}\ s^{-1}$) and a large exciton binding energy of 60 meV [24]. Moreover, the electron injection efficiency of ZnO is almost equivalent to that of $TiO_2$. The electron lifetime of ZnO is significantly higher, and the recombination rate is lower than $TiO_2$. Nevertheless, ZnO-based DSSCs also have suffered from chemical instability in acidic electrolytes and thereby showed slow electron injection kinetics from dye to ZnO photoanode due to the formation of an insulating surface agglomeration layer. Alternatively, tin oxide ($SnO_2$) can be a good choice as it is an *n*-type and wide bandgap semiconductor with excellent optical and electrical properties compared to $TiO_2$. The electron mobility in $SnO_2$ (~100–250 $cm^2\ V^{-1}\ s^{-1}$) is two orders of magnitude higher than $TiO_2$ (~0.1–1.0 $cm^2\ V^{-1}\ s^{-1}$), suggesting a faster diffusion transport of the photo-induced electrons. Secondly, $SnO_2$ has a higher bandgap (3.4 eV) than anatase $TiO_2$ (3.2 eV), which creates fewer oxidative holes in the valence band (fewer oxidative holes facilitate long-term stability and higher stability under long-term UV irradiation) [25]. The Niobium oxide ($Nb_2O_5$) is another wide bandgap semiconductor with 3.49 eV bandgap energy, which is nearly 0.29 eV larger than that of $TiO_2$ (anatase). Because of its larger bandgap and higher conduction band edge compared with anatase $TiO_2$ it is used to achieve relatively higher $V_{oc}$ than anatase $TiO_2$ [26]. Recently, Tungsten oxide ($WO_3$) has attracted immense attention due to its 2.8 eV bandgap energy, which would theoretically utilize ~12% of incident solar light of the visible region. In comparison with $TiO_2$, $WO_3$ possesses a higher mobility and has its conduction band edge at a more-positive location (~0.5 V). Therefore, it is speculated that the $V_{oc}$ in $WO_3$ nanostructured electrode is limited due to the lower difference between its conduction band and redox potential of electrolytes [27]. Bismuth oxide ($Bi_2O_3$) has several advantages due to its unique electrical, optical, and mechanical properties. It exists in four crystal phases, i.e., monoclinic α-$Bi_2O_3$, tetragonal β-$Bi_2O_3$, cubic γ-$Bi_2O_3$, and cubic δ-$Bi_2O_3$. The α-$Bi_2O_3$ phase is most stable at low temperatures up to 730°C, while δ-$Bi_2O_3$ phase is stable when the temperature is above 1000 K. The β-$Bi_2O_3$ and γ-$Bi_2O_3$ phases are high-temperature metastable phases. The $Bi_2O_3$ also exhibits a high refractive index, dielectric permittivity, high oxygen ion conductivity, and remarkable photoconductivity and photoluminescence [28]. Its bandgap energy of 2.5–3.1 eV mostly depends on the crystal phase type. The narrow bandgap of $Bi_2O_3$ makes it suitable for a large range of applications including optical coatings, photovoltaics, microwave-integrated circuits, superconductor, etc.

### 4.2 Ternary transition metal oxides

Besides the simple binary metal oxide systems, ternary metal oxide systems such as Strontium titanate ($SrTiO_3$), Zinc Stannate ($Zn_2SnO_4$), and Barium Stannate ($BaSnO_3$) have also been considered as photoanode materials in the DSSCs and PSCs (**Figure 4b**). The $SrTiO_3$ is a semiconductor with bandgap similar of 3.2 eV. However, its conduction band is relatively at higher position than that of $TiO_2$, which results in a higher $V_{oc}$ [29]. A high dielectric constant makes $SrTiO_3$ as electrically mesoporous even with a large particle size of ~80 nm [30]. In addition, $Zn_2SnO_4$ is particularly interesting because of its physical and electrical properties. The 3.6 eV bandgap and 10–15 $cm^2\ V^{-1}\ s^{-1}$ electron mobility of $Zn_2SnO_4$ have made it stable against UV light with high, electrical conductivity, and low visible absorption over $TiO_2$ [31]. The ternary $BaSnO_3$ is an *n*-type semiconductor with a wide bandgap of 3.1 eV, and its band structure and electrical properties can be controlled easily by atomic substitution or doping into the Ba or Sn site for better performance when used in DSSCs' application [32]. In this sense, as the electrode materials in DSSCs, the ternary oxides are better than the binary.

## 5. Conclusions

The DSSC and PSC solar cells have attracted scientific and technological importance as an alternative to conventional Si-based solar cells. A market feasibility of the solar cells will be a part of the manufacturing cost, durability, fabrication time, chemical stability, mechanical robustness, and power conversion efficiency. The design strategy, preparation method, and surface chemistry of transition metal oxides with excellent electrical and optical properties will also have an impact. An era of nanotechnology has opened a door to tailing transition metal oxide materials for DSSCs' and PSCs' applications. In this chapter, we briefly have discussed four basic topics about the DSSCs and PSCs. Initially, background, motivation, and present needs of DSSCs and PSCs are covered. The required photovoltaic parameters including short-circuit current density, open-circuit voltage, fill factor, and incident photon-to-current conversion efficiency to develop good DSSCs and PSCs are emphasized in brief. The historical background has been presented to get an idea regarding the new investigations taking place to replace dye molecules through perovskite absorber layer. Information on the theoretical and practical details has also been provided to obtain DSSCs and PSCs with high solar-to-electricity power conversion efficiencies. Working principle of the DSSCs is explored by considering electron and hole pair generation, charge transportation, and charge separation and recombination etc. In transition metal oxide in binary and ternary forms like zero, one, two, and three dimensions such as nanoparticles, nanotubes, nanodisks, and nanoflowers, their implication is proposed as good candidates in developing a smart and wearable DSSCs and PSCs in the future.

## Acknowledgements

Author SFS would like to thank University Grants Commission, New Delhi, for awarding Dr. D. S. Kothari Postdoctoral Fellowship scheme (F.4-2/2006 (BSR)/CH/16-17/0015) and author KHK would like to thank Global Frontier Program through the Global Frontier Hybrid Interface Materials (GFHIM) of the National Research Foundation of Korea (NRF) funded by the Ministry of Science, ICT & Future Planning (2013M3A6B1078874).

## Conflict of interest

The authors declare no competing interests.

## Notes/thanks/other declarations

Authors SFS and RSM would like to thank Mr. S. S. Sangale and Mr. Y. T. Nakate for arranging the references and designing the cartoon images.

## Acronyms and abbreviations

| | |
|---|---|
| AM | Air mass |
| DSSCs | Dye-sensitized solar cells |
| $e^-$ | Electron |
| $E_g$ | Bandgap |
| EQE | External quantum efficiency |
| *ff* | Fill factor |
| FTO | Fluorine-tin-oxide |
| $h^+$ | Hole |
| HOMO | Highest occupied molecular orbital |
| I-V | Current-voltage |
| IPCE | Incident photon-to-current conversion efficiency |
| $I_{mp}$ | Current at maximum power |
| $J_{sc}$ | Short-circuit current density |
| $J$ | Photocurrent density |
| LUMO | Lowest unoccupied molecular orbital |
| $\eta$ | Solar-to-electrical power conversion efficiency |
| OPVs | Organic Photovoltaic Cells |
| PSCs | Perovskite solar cells |
| $P$ | Power |
| QD-DSSCs | Quantum dot-sensitized solar cells |
| Si-SCs | Silicon solar cells |
| $V_{oc}$ | Open-circuit voltage |
| VB | Valence band |
| $V_{mp}$ | Voltage at maximum power |
| $\lambda$ | Wavelength |

## Author details

Shoyebmohamad F. Shaikh[1,2], Nanasaheb M. Shinde[3], Damin Lee[3], Abdullah M. Al-Enizi[2], Kwang Ho Kim[3] and Rajaram S. Mane[1*]

1 School of Physical Sciences, Swami Ramanand Teerth Marathwada University, Nanded, MH, India

2 Chemistry Department, College of Sciences, King Saud University, Riyadh, Saudi Arabia

3 National Core Research Center, Pusan National University, Busan, Republic of Korea

*Address all correspondence to: rajarammane70@srtmun.ac.in and kwhokim@pusan.ac.kr

## References

[1] Gratzel M. Photoelectrochemical cell. Nature. 2001;**414**:338-344. DOI: 10.1038/35104607

[2] Shah A, Torres P, Tscharner R, Wyrsch N, Keppner H. Photovoltaic technology: The case for thin-film solar cells. Science. 1999;**285**:692-698. DOI: 10.1126/science.285.5428.692

[3] Reynolds DC, Leies G, Antes LL, Marburger RE. Photovoltaic effect in cadmium sulfide. Physics Review. 1954;**96**:533-534. DOI: https://doi.org/10.1103/PhysRev.96.533

[4] Hua Y. Modification of $TiO_2$ photoanodes for dye-sensitized solar cells [thesis]. Griffith School of Environment Science, Environment, Engineering and Technology: Griffith University; 2010

[5] Flynn BW, Owen AE, Mavor J. Dye-sensitized of the photoconductivity of $SiO_2$ films in M-dye-$SiO_2$-M structure. Journal of Physics C: Solid State Physics. 1977;**10**:4051-4059. DOI: 10.1088/0022-3719/10/20/013

[6] Oregan B, Gratzel M. A low-cost, high efficiency solar cell based on dye-sensitized colloidal $TiO_2$ films. Nature. 1991;**353**:737-739. DOI: 10.1038/353737a0

[7] Bach U, Lupo D, Comte P, Moser JE, Weissortel F, Salbeck J, et al. Solid-state dye-sensitized mesoporous $TiO_2$ solar cells with high photon-to-electron conversion efficiencies. Nature. 1998;**395**:583-585. DOI: 10.1038/26936

[8] Burschka J, Dualeh A, Kessler F, Baranoff E, Cevey-Ha NL, Yi C, et al. Tris (2-(1 H-pyrazol-1-yl) pyridine) cobalt (III) as p-type dopant for organic semiconductors and its application in highly efficient solid-state dye-sensitized solar cells. Journal of the American Chemical Society. 2011;**133**:18042-18045. DOI: 10.1021/ja207367t

[9] Kojima A, Teshima K, Shirai Y, Miyasaka T. Organometal halide perovskites as visible-light sensitizers for photovoltaic cells. Journal of the American Chemical Society. 2009;**131**:6050-6051. DOI: 10.1021/ja809598r

[10] Im JH, Lee CR, Lee JW, Park SW, Park NG. 6.5% efficient perovskite quantum-dot-sensitized solar cell. Nanoscale. 2011;**3**:4088-4093. DOI: 10.1039/C1NR10867K

[11] Kim H, Lee C, Im J, Lee K, Moehl T, Marchioro A, et al. Lead iodide perovskite sensitized all-solid-state submicron thin film mesoscopic solar cell with efficiency exceeding 9%. Scientific Reports. 2012;**2**:591. DOI: 10.1038/srep00591

[12] Jeon NJ, Noh JH, Kim YC, Yang WS, Ryu S, Seok SI. Solvent engineering for high-performance inorganic-organic hybrid perovskite solar cells. Nature Materials. 2014;**13**:897-903. DOI: 10.1038/nmat4014

[13] Yang W, Noh J, Jeon N, Kim Y, Ryu S, Seo J, et al. High-performance photovoltaic perovskite layers fabricated through intramolecular exchange. Science. 2015;**348**:1234-1237. DOI: 10.1126/science.aaa9272

[14] Sahli F, Werner J, Kamino A, Bräuninger M, Monnard R, Paviet-Salomon B, et al. Fully textured monolithic perovskite/silicon tandem solar cells with 25.2% power conversion efficiency. Nature Materials. 2018;**1**:820-826. DOI: 10.1038/s41563-018-0115-4

[15] Shaikh SF. Chemical synthesis of metal oxides for DSSCS application: Effect of interfacial surface modification on power conversion

efficiency [thesis]. Clean Energy and Chemical Engineering, University of Science and Technology; 2015

[16] Nazeeruddin Md K, Baranoff E, Gratzel M. Dye-sensitized solar cells: A brief overview. Solar Energy. 2011;**85**:1172-1178. DOI: 10.1016/j.solener.2011.01.018

[17] Tiwari JN, Tiwari RN, Kim KS. Zero-dimensional, one-dimensional, two-dimensional and three-dimensional nanostructured materials for advanced electrochemical energy devices. Progress in Materials Science. 2012;**57**:724-803. DOI: 10.1016/j.pmatsci.2011.08.003

[18] Kim YT, Han JH, Hong BH, Kwon YU. Electrochemical synthesis of CdSe quantum-dot arrays on a graphene basal plane using mesoporous silica thin-film templates. Advanced Materials. 2010;**22**(4):515-518. DOI: https://doi.org/10.1002/adma.200902736

[19] Kim WY, Choi YC, Kim KS. Understanding structures and electronic/spintronic properties of single molecules, nanowires, nanotubes, and nanoribbons towards the design of nano devices. Journal of Materials Chemistry. 2008;**18**(38):4510-4521. DOI: 10.1039/B804359K

[20] Jung SH, Oh E, Lee KH, Yang Y, Park CG, Park W, et al. Sonochemical preparation of shape-selective ZnO nanostructures. Crystal Growth and Design. 2007;**8**(1):265-269. DOI: 10.1021/cg070296l

[21] Ahn JH, Kim HS, Lee KJ, Jeon S, Kang SJ, Sun Y, et al. Heterogeneous three-dimensional electronics by use of printed semiconductor nanomaterials. Science. 2006;**314**(5806):1754-1757. DOI: 10.1126/science.1132394

[22] Luo H, Takata T, Lee Y, Zhao J, Domen K, Yan Y. Photocatalytic activity enhancing for titanium dioxide by co-doping with bromine and chlorine. Chemistry of Materials. 2004;**16**:846-849. DOI: 10.1021/cm035090w

[23] Shaikh SF, Mane RS, Min BK, Hwang YJ, Joo OS. D-sorbitol-induced phase control of $TiO_2$ nanoparticles and its application for dye-sensitized solar cells. Scientific Reports. 2016;**6**:20103. DOI: 10.1038/srep20103

[24] Zheng YZ, Tao X, Hou Q, Wang DT, Zhou WL, Chen JF. Iodine-doped ZnO nanocrystalline aggregates for improved dye-sensitized solar cells. Chemistry of Materials. 2011;**23**:3-5. DOI: 10.1021/cm101525p

[25] Shaikh SF, Mane RS, Joo OS. Mass scale sugar-mediated green synthesis and DSSCs application of tin oxide nanostructured photoanode: Effect of zinc sulphide layering on charge collection efficiency. Electrochimica Acta. 2014;**147**:408-417. DOI: 10.1016/j.electacta.2014.08.146

[26] Lenzmann F, Krueger J, Burnside S, Brooks K, Gratzel M, Gal D, et al. Surface photovoltage spectroscopy of dye-sensitized solar cells with $TiO_2$, $Nb_2O_5$, and $SrTiO_3$ nanocrystalline photoanodes: Indication for electron injection from higher excited dye states. The Journal of Physical Chemistry. B. 2001;**10**:6347-6352. DOI: 10.1021/jp010380q

[27] Hara K, Zhao Z, Cui Y, Miyauchi M, Miyashita M, Mori S. Nanocrystalline electrodes based on nanoporous-walled $WO_3$ nanotubes for organic-dye sensitized solar cells. Langmuir. 2011;**27**:12730-12736. DOI: 10.1021/la201639f

[28] Shaikh SF, Rahman G, Mane RS, Joo OS. Bismuth oxide nanoplates-based efficient DSSCs: Influence of ZnO surface passivation layer. Electrochimica Acta. 2013;**111**:593-600. DOI: 10.1016/j.electacta.2013.08.066

[29] Sun Q, Hong Y, Zang T, Liu Q, Yu L, Dong L. The application of heterostructured $SrTiO_3$-$TiO_2$ nanotube arrays in dye-sensitized solar cells. Journal of the Electrochemical Society. 2018;**165**(4):H3069-H3075. DOI: 10.1149/2.0101804jes

[30] Hod I, Shalom M, Tachan Z, Rühle S, Zaban A. $SrTiO_3$ recombination-inhibiting barrier layer for type II dye-sensitized solar cells. Journal of Physical Chemistry C. 2010;**114**:10015-10018. DOI: 10.1021/jp101097j

[31] Chen J, Lu L, Wang W. $Zn_2SnO_4$ nanowires as photoanode for dye sensitized solar cells and the improvement on open-circuit voltage. Journal of Physical Chemistry C. 2012;**116**:10841-10847. DOI: 10.1021/jp301770n

[32] Shin SS, Kim JS, Suk JH, Lee KD, Kim DW, Park JH, et al. Improved quantum efficiency of highly efficient perovskite $BaSnO_3$-based dye-sensitized solar cells. ACS Nano. 2013;**7**:1027-1035. DOI: 10.1021/nn305341x